

LETTER • **OPEN ACCESS**

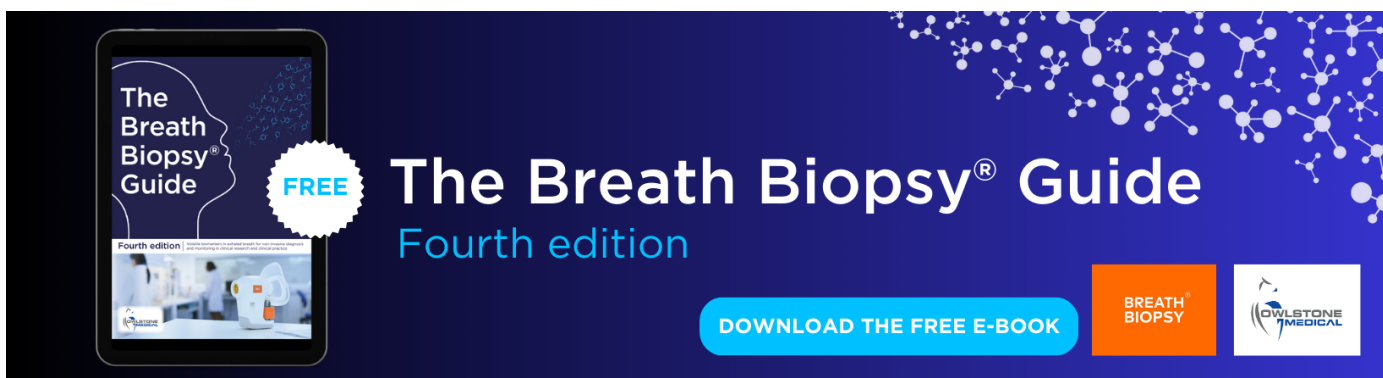
## Summer heat extremes in northern continents linked to developing ENSO events

To cite this article: Ming Luo and Ngar-Cheung Lau 2020 *Environ. Res. Lett.* **15** 074042

View the [article online](#) for updates and enhancements.

You may also like

- [The Impact of Two Types of ENSO Events on Tropical Cyclones in the Northwest Pacific](#)  
Zhiwei Chen, Jiancheng Kang, Guodong Wang et al.
- [ENSO prediction based on Long Short-Term Memory \(LSTM\)](#)  
Cao Xiaoqun, Guo Yanan, Liu Bainian et al.
- [Southwest US winter precipitation variability: reviewing the role of oceanic teleconnections](#)  
J Karanja, B M Svoma, J Walter et al.



The Breath Biopsy® Guide  
Fourth edition

FREE

DOWNLOAD THE FREE E-BOOK

BREATH BIOPSY

OWLSTONE MEDICAL

# Environmental Research Letters



## LETTER

# Summer heat extremes in northern continents linked to developing ENSO events

### OPEN ACCESS

RECEIVED  
28 December 2019

REVISED  
3 March 2020

ACCEPTED FOR PUBLICATION  
5 March 2020

PUBLISHED  
6 July 2020

Original content from this work may be used under the terms of the [Creative Commons Attribution 4.0 licence](https://creativecommons.org/licenses/by/4.0/).

Any further distribution of this work must maintain attribution to the author(s) and the title of the work, journal citation and DOI.



Ming Luo<sup>1,2,4</sup>  and Ngar-Cheung Lau<sup>2,3</sup>

<sup>1</sup> School of Geography and Planning, and Guangdong Key Laboratory for Urbanization and Geo-simulation, Sun Yat-sen University, Guangzhou 510275, People's Republic of China

<sup>2</sup> Institute of Environment, Energy and Sustainability, The Chinese University of Hong Kong, Sha Tin, N.T., Hong Kong Special Administrative Region of China, People's Republic of China

<sup>3</sup> Department of Geography and Resource Management, The Chinese University of Hong Kong, Sha Tin, N.T., Hong Kong Special Administrative Region of China, People's Republic of China

<sup>4</sup> Author to whom any correspondence should be addressed.

E-mail: [luo.ming@hotmail.com](mailto:luo.ming@hotmail.com)

**Keywords:** summer heat extremes, El Niño-Southern Oscillation, interannual variability, circumglobal teleconnection, jet stream

## Abstract

Understanding the variations of extreme weather/climate events is important to improve the seasonal forecast skill of such harmful events. Previous studies have linked boreal summer hot extremes to decaying El Niño-Southern Oscillation (ENSO) events at the interannual scale, but how these hot extreme episodes respond to developing ENSO events remains unclear. Using observational analyses, we demonstrate strong linkages between developing ENSO and extreme heat events in northern continents. In particular, heat extremes in North America, Eastern Europe–Central Asia and Northeast Asia tend to be more frequent during La Niña developing summers and less frequent during El Niño developing phases. Associated atmospheric changes reveal that developing ENSO events feature a circumglobal teleconnection (CGT) pattern over the mid-latitudes. In the La Niña developing summer, this CGT pattern exhibits enhanced geopotential height and anomalous anticyclones over North Pacific, North America, Eastern Europe–Central Asia and Northeastern Asia, and the jet stream generally shifts northward. The atmospheric circulation changes lead to more persistent weather conditions that favor extreme heat events in mid-latitudes. Conversely, opposite changes associated with developing El Niño can inhibit heat extremes in the above locations. The responses of heat extremes to different types (i.e., conventional Eastern Pacific and Modoki Central Pacific) and durations (1 and 2 year) of ENSO events are also discussed.

## 1. Introduction

As one of the most harmful extreme climate and weather phenomena, summer extreme heat events have been shown to exert severe influences on human health and the eco-system (Easterling *et al* 2000, Kovats and Hajat 2008, Deschênes and Greenstone 2011, Ma *et al* 2014, Gasparrini *et al* 2015, Forzieri *et al* 2017). Heat extremes have been intensifying over the past decades, and their frequency of occurrence is projected to increase still further in the coming decades under global warming, thus posing increasing threats to human society and the natural environment (Meehl and Tebaldi 2004, IPCC 2013, Dosio *et al* 2018). At the regional scale, rapid urbanization

and land use may further accelerate the increasing tendency in hot extremes in many regions such as China and North America (Oleson *et al* 2015, Sun *et al* 2016, Freychet *et al* 2017, Luo and Lau 2017, Luo and Lau 2019a).

In addition to their long-term trends, the interannual variations of summer heat extremes at a shorter time scale are closely linked with prominent modes of climate variability. For instance, the westward extension of the western North Pacific (WNP) subtropical high plays an important role in modulating heat waves in eastern and southern China (Ding *et al* 2010, Luo and Lau 2017, Liu *et al* 2019a). The changes in the East Asian jet stream and the South Asian high are also linked with the variability of

summer heat extremes in China (Wang *et al* 2013, 2014). Particularly noteworthy among the modes of climate variability is the El Niño–Southern Oscillation (ENSO), which is an important interannual-scale phenomenon that has remarkable influences on the mean seasonal climate around the world (Wu *et al* 2003, Zhao *et al* 2019, Rao and Ren 2020). Different ENSO phases, intensities and flavors may induce distinct climate anomalies in remote regions through large-scale atmospheric changes (Zhao *et al* 2019). ENSO may also exert impacts on extreme climate and weather events, as extreme temperature events are often caused by the changes in atmospheric circulation (e.g. blockings), which can be influenced by the underlying sea surface temperature (SST) anomalies associated with ENSO (Kenyon and Hegerl 2008, Alexander *et al* 2009, Arblaster and Alexander 2012, Sun *et al* 2015, Gao *et al* 2020a). Recent studies revealed that ENSO events also have profound effects on the stratosphere (Garfinkel and Hartmann 2007, Rao and Ren 2016, 2017). In particular, the stratospheric sudden warming events are modulated by ENSO through the upward propagation of planetary waves from the troposphere (Barriopedro and Calvo 2014, Liu *et al* 2019b).

ENSO has prominent effects on hot extremes and heatwaves in many parts of the world such as North America (Loikith and Broccoli 2014), East Asia (Luo and Lau 2019b, Yeo *et al* 2019, Gao *et al* 2020b), Southeast Asia (Lin *et al* 2018), Australia (Loughran *et al* 2019), Canada and South Africa (Kenyon and Hegerl 2008, Arblaster and Alexander 2012). The probabilities of warm summer days and months over Mexico and the south-central United States are significantly increased in the El Niño decaying summer (Loikith and Broccoli 2014). Behera *et al* (2013) found that the transition phase from El Niño to La Niña is accompanied by more frequent extreme heat events in Eastern Europe. Our previous study also suggests that heatwaves in southern and eastern China tend to be intensified during the summers of decaying El Niño, and weakened during decaying La Niña phase (Luo and Lau 2019a). The WNP subtropical high and anticyclone play a role in these relationships (Luo and Lau 2019). El Niño forcing can also lead to more frequent extreme temperature episodes in Australia through several mechanisms such as the heat advection from lower latitudes via a moving high-pressure system, the boundary layer diabatic heating by the land surface, and the subsidence of air with high potential temperature (Loughran *et al* 2019).

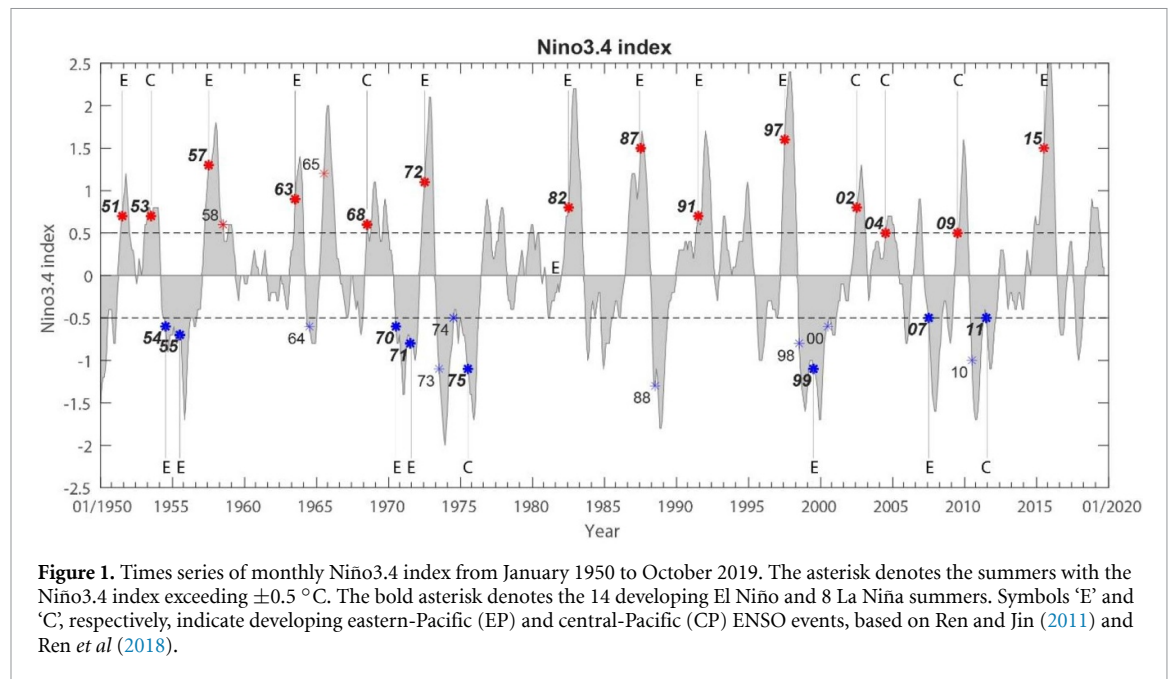
However, the above studies mainly focused on the changes in summer heat extremes responding to preceding El Niño/La Niña events (i.e. decaying summers). Linkages between heat extremes and developing ENSO remain to be documented in detail, and the causes for such linkages remain to be identified. Also, previous studies have shown that developing

and decaying ENSO events are associated with distinctive summer circulation patterns and may pose different influences on climate in remote regions (Lin and Li 2008, Wu *et al* 2009, Kosaka *et al* 2012, Rao and Ren 2017, Xue *et al* 2018, Wen *et al* 2019, Zhao *et al* 2019). These considerations suggest that developing and decaying ENSO events may have different linkages with summer heat extreme events. The goal of the current study is, therefore, to extend previous studies by examining the possible linkages between summer heat extremes in northern continents and developing La Niña/El Niño events.

## 2. Data and methods

In this study, two different measures of summer extreme heat events defined by the Expert Team on Climate Change and Indices (ETCCDI), namely daytime TX90p and nighttime TN90p, are examined. TX90p (TN90p) is defined as the number of days when the daily maximum (minimum) temperature exceeds its 90th percentile value. The percentile values are computed from daily maximum ( $T_{max}$ ) and minimum ( $T_{min}$ ) temperatures, respectively, in the reference period 1961–1990. TX90p and TN90p can thereby be used to measure daytime and nighttime heat extremes, respectively. The monthly statistics of TX90p and TN90p frequencies over northern continents in the summers (June–August, or JJA) of 1951–2019 are from the global land gridded GHCNDEX dataset of climate extremes (Donat *et al* 2013), which is available at [www.climdex.org](http://www.climdex.org) and has a spatial resolution of  $2.5^\circ \times 2.5^\circ$ . In order to reveal the associated atmospheric circulation changes in response to developing ENSO events, monthly fields of geopotential height and horizontal winds are obtained from the NCEP/NCAR Reanalysis I dataset (Kalnay *et al* 1996).

ENSO events are defined by the monthly Niño3.4 index (figure 1). This index is collected from the NOAA Climate Prediction Center at its website [http://www.cpc.noaa.gov/products/analysis\\_monitoring/ensostuff/ensoyears.shtml](http://www.cpc.noaa.gov/products/analysis_monitoring/ensostuff/ensoyears.shtml). Following Wu *et al* (2009) and Wen *et al* (2019), an ENSO developing summer is defined when the absolute value of the JJA Niño3.4 index exceeds  $0.5^\circ\text{C}$  and ENSO reaches a mature phase in the following winter. Here, a mature ENSO event is defined when the 3 month Niño3.4 index exceeds  $\pm 0.5$  for at least five consecutive months (Trenberth 1997). Due to the complexity of ENSO evolution patterns, we exclude 1958, 1964, 1965, 1973, 1988, 1998, 2000, 2011, as these summers are preceded by a strong El Niño/La Niña events in the previous winter. Out of 68 summers in the period of 1951–2019, 14 developing El Niño summers and 8 developing La Niña summers are extracted for subsequent analysis. The identification of developing ENSO summers is illustrated in figure 1. Note that when the mixed events are included for composite



analysis, the results show only marginal differences from that presented in the following section. Several above-identified developing years such as 1955, 1975, 1958, 1999 and 2011 also follow a previous 'developing' event. When these years are excluded, the results also show little change from when these years are included (not shown). We thus keep these developing years in the following investigations.

The atmospheric patterns associated with developing ENSO events are revealed by examining the composite maps for the differences in the detrended anomalies of the related atmospheric variables between the developing La Niña and El Niño summers (i.e. La Niña minus El Niño). The significance of the differences at the 0.05 level is evaluated by the Student's t-test, which has been widely used in examining the ENSO effects in previous studies (e.g. Pozo-Vázquez *et al* (2001), Philippon *et al* (2012), Karori *et al* (2013), Choi *et al* (2019)). The anomalies of the related atmospheric variables are calculated by removing the climatological mean over the period of 1961–1990. The long-term variations in these variables and in the frequency of summer extreme heat events are removed by using the 9 year high pass Lanczos filtering (Duchon 1979).

### 3. Results

#### 3.1. Changes in summer heat extremes associated with developing ENSO events

The differences in summer TX90p and TN90p frequencies (with the trends removed by a high-pass filter) over northern continents between the La Niña and El Niño developing summers are presented in figure 2. These charts illustrate that summer extreme heat events exhibit strong differences between developing El Niño and La Niña events. During the developing summer of La Niña (El

Niño), the frequencies of TX90p and TN90p generally increase (decrease) over the middle latitudes of northern continents. In the developing phase of La Niña (El Niño) events, significant increases (decreases) in the frequency of summer extreme heat events occur in North America, Eastern Europe–Central Asia, and Northeast Asia (as denoted by dashed boxes in figure 2); whereas anomalies of the opposite polarity are found over parts of northwestern North America and central China for TX90p (figure 2(a)).

We calculate the correlation coefficient between the JJA Niño3.4 index and the high-pass filtered frequency of heat events over North America, Eastern Europe–Central Asia, and Northeast Asia (table 1). These regions are chosen as they exhibit the most prominent anomalies during developing ENSO summers (see figure 2). The Niño3.4 index is correlated with summer TX90p (TN90p) frequencies in North America, Eastern Europe–Central Asia, and Northeast Asia at levels of  $-0.41$  ( $-0.43$ ),  $-0.28$  ( $-0.28$ ), and  $-0.34$  ( $-0.42$ ), respectively. These coefficients are all statistically significant at the 0.05 level. These results demonstrate that the developing ENSO events have strong linkages with summer hot weather in these mid-latitude regions. A developing La Niña event is linked to increased heat extremes in these regions, while a developing El Niño is associated with decreased heat events.

To further demonstrate the relationships between ENSO and hot extremes over the midlatitudes of the Northern Hemisphere, we also present the scatter plots of the TX90p/TN90p frequencies versus the Niño3.4 index for individual years in figure 3. As it shows, the Niño3.4–TX90p/TN90p relationships are evident in a large majority of the individual ENSO events being considered. The Niño3.4 index exhibits negative correlations (i.e. statistically significant at the 0.05 level; see also table 1) with the

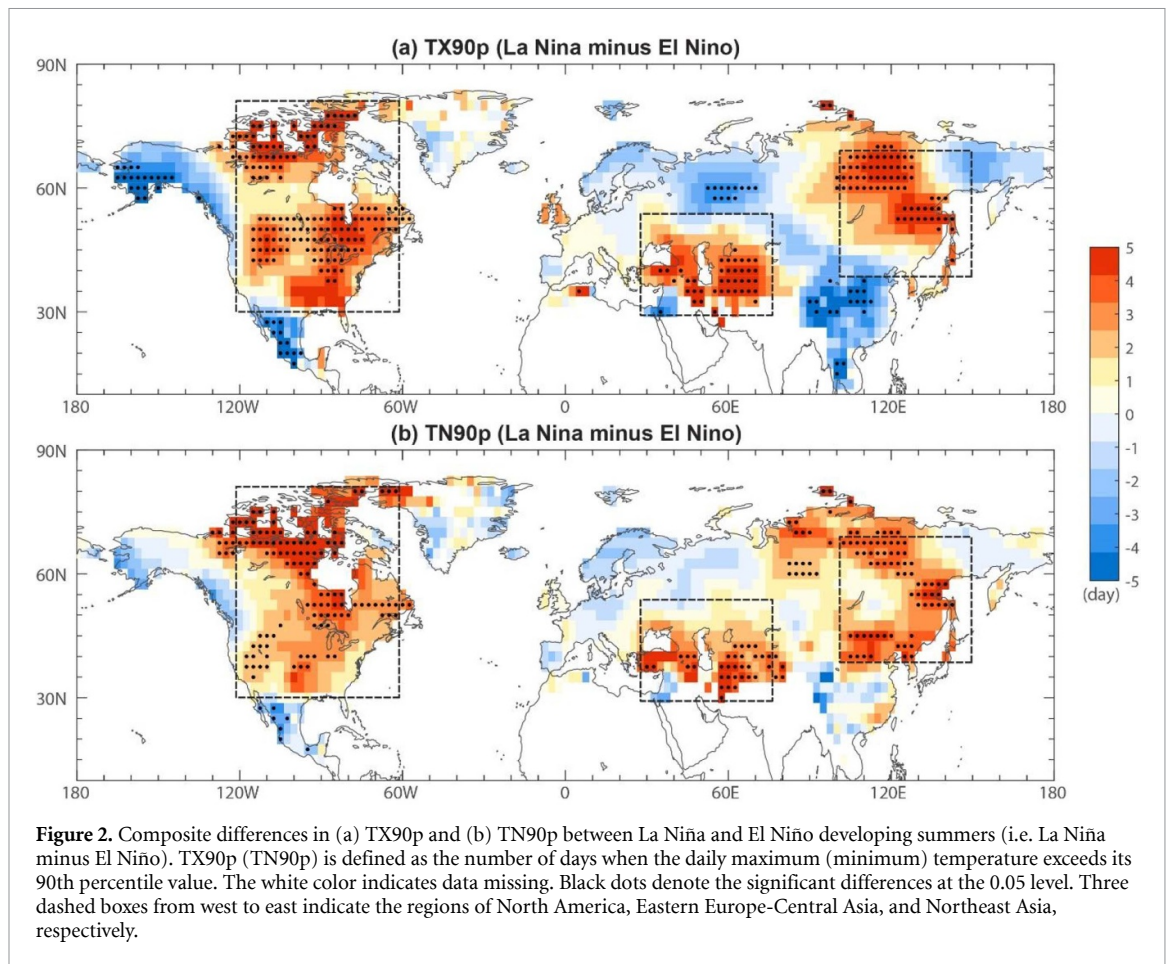


**Figure 2.** Composite differences in (a) TX90p and (b) TN90p between La Niña and El Niño developing summers (i.e. La Niña minus El Niño). TX90p (TN90p) is defined as the number of days when the daily maximum (minimum) temperature exceeds its 90th percentile value. The white color indicates data missing. Black dots denote the significant differences at the 0.05 level. Three dashed boxes from west to east indicate the regions of North America, Eastern Europe–Central Asia, and Northeast Asia, respectively.

**Table 1.** Correlation coefficients of the JJA Niño3.4 index with summer heat extremes over three subregions of the Northern Hemisphere (i.e. North America, Eastern Europe–Central Asia, and Northeast Asia, as indicated by the boxes in Figure 2) and the mean detrended frequencies of heat extremes (unit: day) during the summers of developing La Niña/El Niño during 1951–2019. All correlation coefficients are significant at the 0.05 level.

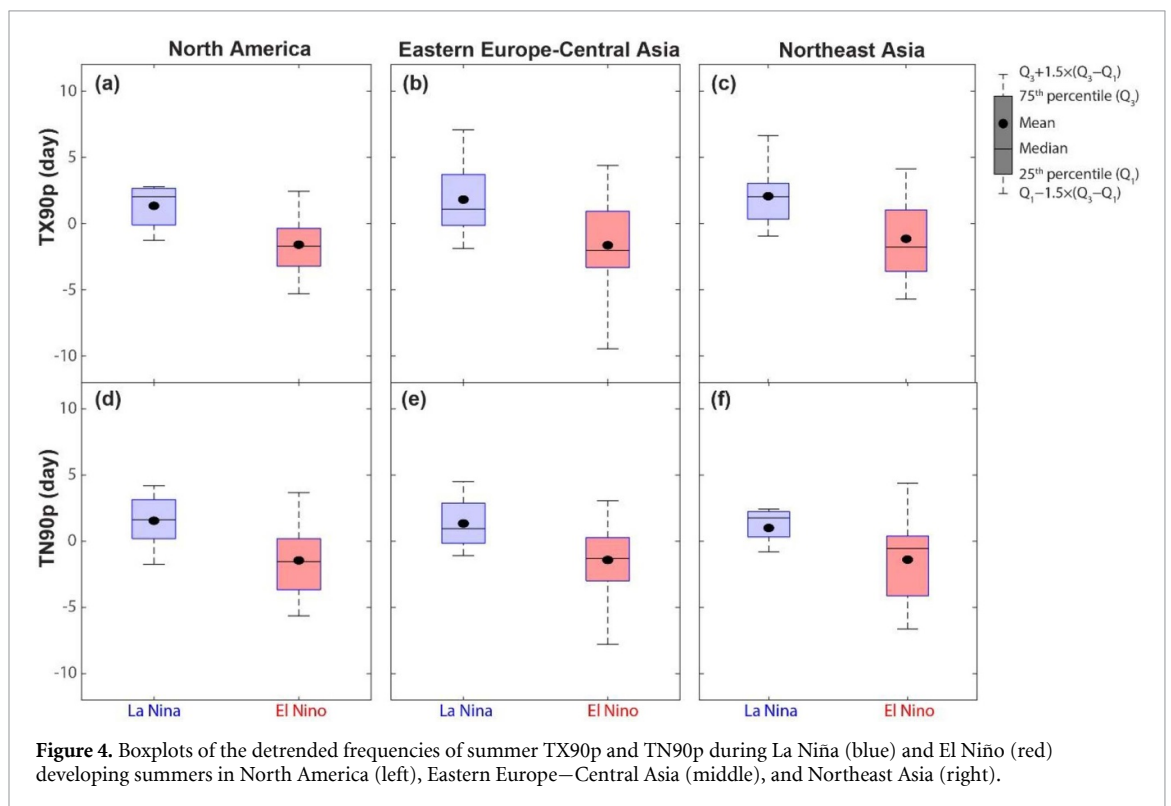
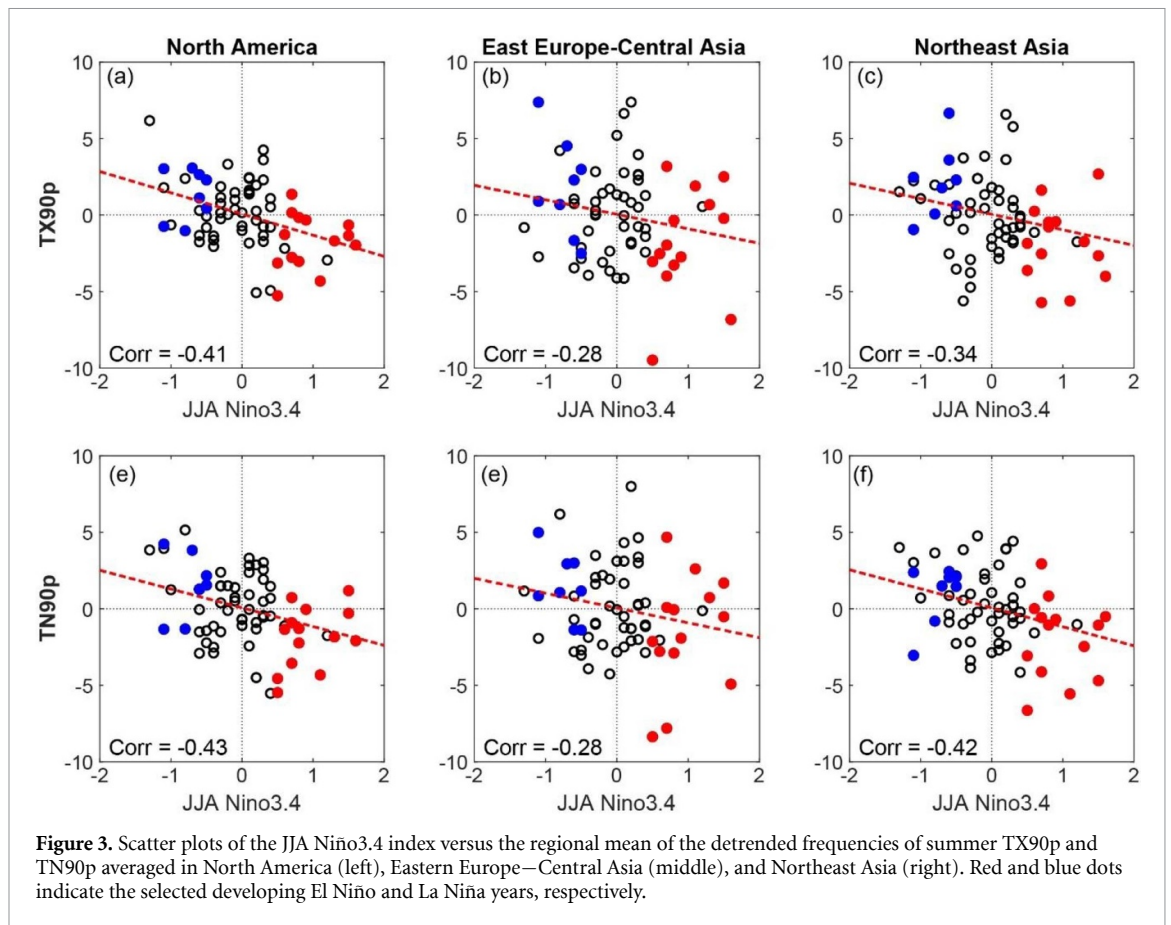
Region	Correlation coefficients with the JJA Niño3.4 index		Frequencies in the summers of developing La Niña/El Niño	
	TX90p	TN90p	TX90p	TN90p
North America	−0.41	−0.43	+1.33/−1.60	+1.55/−1.44
Eastern Europe–Central Asia	−0.28	−0.28	+1.81/−1.64	+1.35/−1.42
Northeast Asia	−0.34	−0.42	+2.07/−1.15	+1.01/−1.39

TX90p/TN90p frequencies, and most developing El Niño (La Niña) events are accompanied by decreased (increased) TX90p/TN90p frequencies.

To highlight the contrast between the La Niña and El Niño developing summers, boxplots of summer TX90p and TN90p frequencies averaged over North American, Eastern Europe–Central Asia, and Northeast Asia are also constructed. The boxplot results are shown in figure 4 and the mean detrended frequencies of summer TX90p and TN90p during the La Niña and El Niño developing summers are tabulated in table 1. Over North America, the regional mean frequency of TX90p (TN90p) is 1.33(1.55) days higher during the summer of developing La Niña and 1.60 (1.44) days lower during the El Niño developing summer. Also, both TX90p and TN90p extremes become more (less) frequent in the La Niña (El Niño)

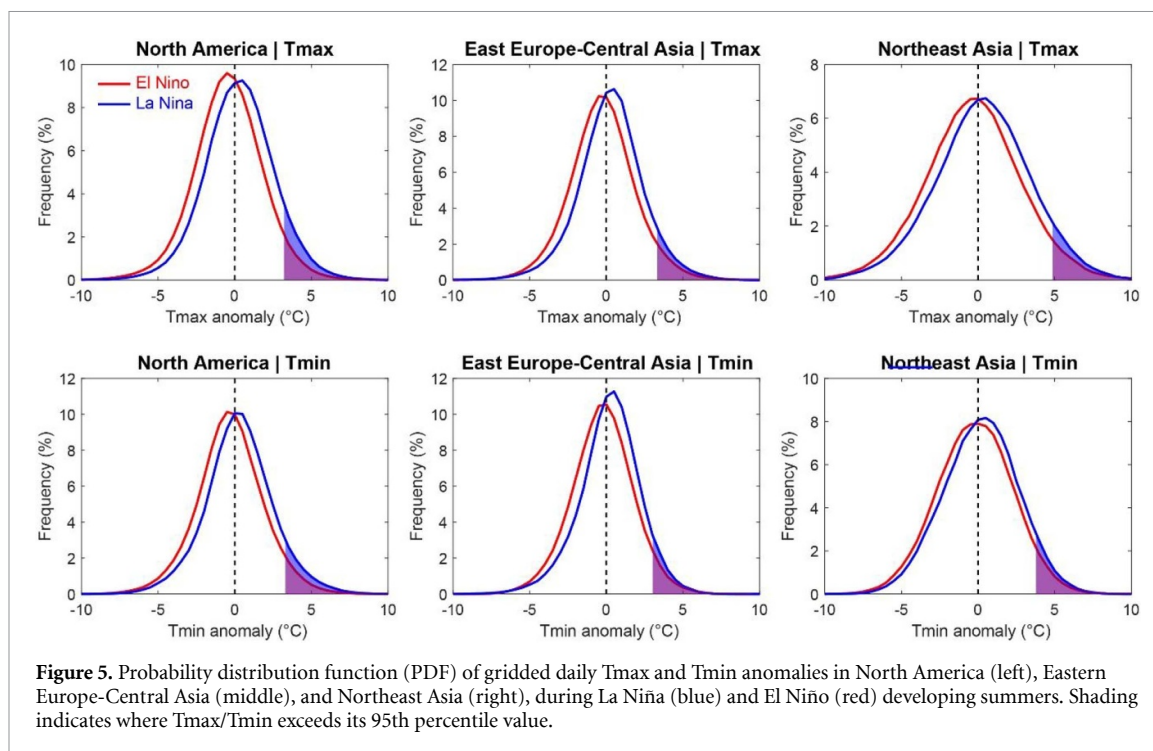
developing summer in Eastern Europe–Central and Northeast Asia.

Figure 5 shows the probability distribution functions (PDFs) of gridded daily Tmax and Tmin anomalies in three selected regions during El Niño and La Niña. The PDF curves of daily Tmax/Tmin anomalies in all three regions during La Niña developing summer (blue curves) tend to be shifted to the right of their counterparts during El Niño (red curves), thus indicating more frequent occurrences of positive temperature anomalies during La Niña as compared to El Niño. On the other hand, the skewness of the red and blue curves are not noticeably different from each other. These findings demonstrate that the more frequent hot extremes during La Niña developing summers than El Niño summers is mainly due to the lateral translation of the distribution curves for



various temperature anomalies, rather than a change in the shape of these distributions. This PDF shift can lead to a dramatic increase in the frequency of high temperature extremes, as shown in the shadings of figure 5. Similar shifts in the distribution of

temperature as a response to ENSO events have also been found by Arblaster and Alexander (2012). By using both observations and model simulations, they showed that the mean and frequency distribution of maximum daily temperature (TXx) in Australia and



the USA are significantly different during El Niño events compared to La Niña events.

### 3.2. Atmospheric circulation changes and physical mechanisms

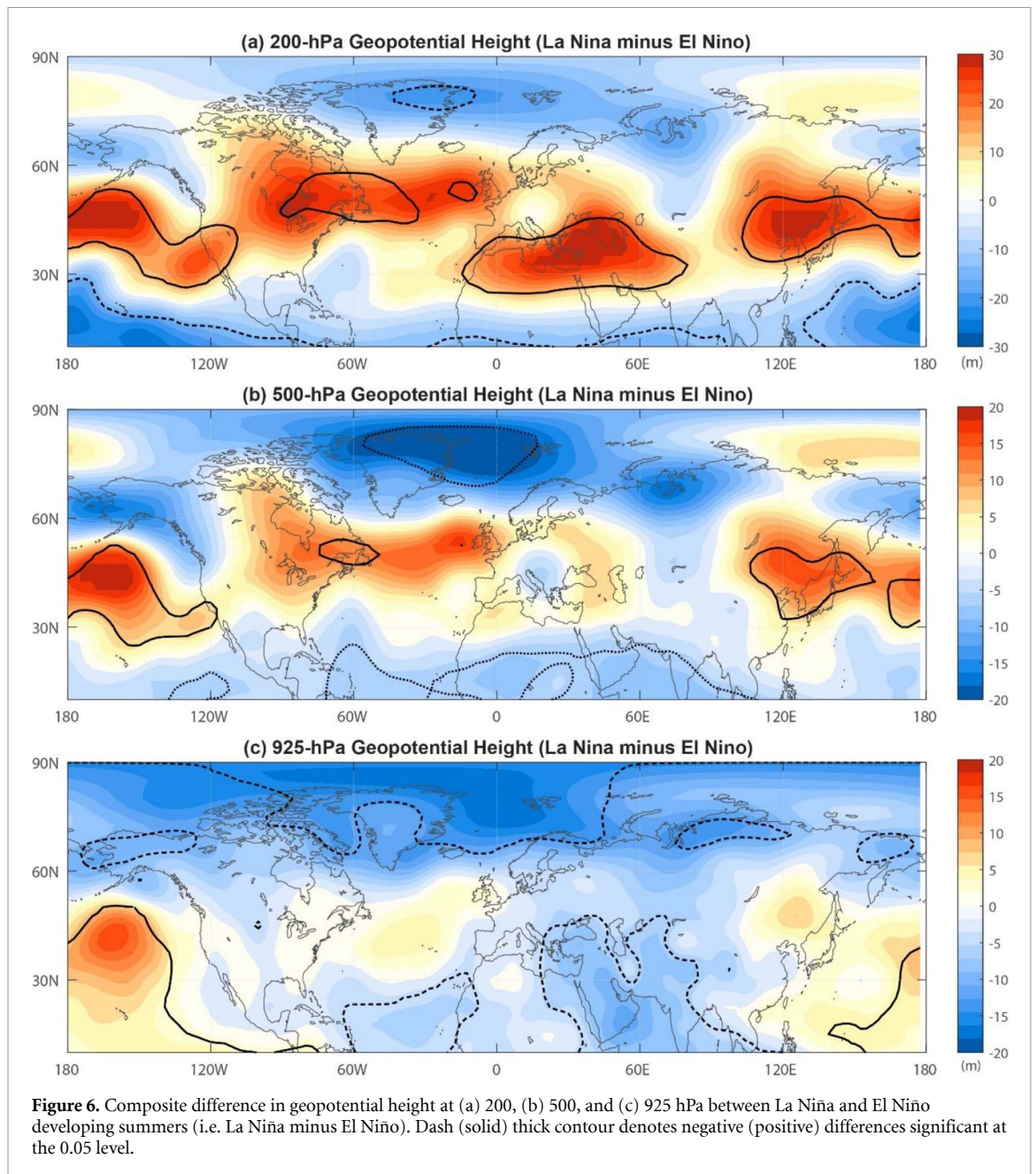
The above results show that many mid-latitude zones of the Northern Hemisphere experience more frequent summer extreme heat weather during La Niña than El Niño developing phases. To highlight the atmospheric circulation changes associated with developing ENSO events, we construct the composite maps for the difference in geopotential height and horizontal wind between the developing La Niña and El Niño summers (i.e. La Niña minus El Niño). These maps can enhance our understanding of how the developing ENSO events are linked to summer extreme heat events in the Northern Hemisphere.

The differences in 200 hPa geopotential height between the developing La Niña and El Niño summers are depicted in figure 6(a). Developing ENSO events are evidently coincident with prominent atmospheric circulation changes in the middle latitudes of the Northern Hemisphere. During developing La Niña (El Niño) events, upper-level height anomalies are predominantly positive (negative) over mid-latitudes, whereas negative (positive) anomalies are discernible over tropical regions and parts of high latitudes. The strongest signals of 200 hPa height in developing ENSO events appear over North America, Central Asia, Northeast Asia, and North Pacific. These sites correspond well with the locations of increased summer heat extremes (recall figure 2). During the summer of developing La Niña (El Niño) events, seasonal mean anomaly pattern tend to be more (less) persistent under the influence of positive (negative)

height anomalies, thus increasing (decreasing) the probability of extreme weather events such as heat-waves and drought (Lau and Nath 2012, Stefanon *et al* 2012, Schaller *et al* 2018).

It is also noted that the positive height anomaly centers appearing over the northern mid-latitudes and extending from North Pacific, North America, Eastern Europe–Central Asia, and Northeast Asia, collectively constitute a zonal wave-like pattern along the westerly jet (figure 6(a)). This zonal feature resembles the circumglobal teleconnection (CGT) pattern during boreal summer, one of the dominant modes of interannual variability in the upper troposphere in the northern extratropics (Ding and Wang 2005). It has been suggested that the CGT pattern is linked to positive rainfall anomalies over the Indian summer monsoon region and that a positive CGT pattern likely occurs during a developing La Niña summer (Ding and Wang 2005, Ding *et al* 2011, Lee *et al* 2014). CGT is strongly influenced by the ENSO cycle in the summer of developing La Niña or El Niña events, especially in recent decades after the 1970s (Wang *et al* 2012, Lee and Ha 2015). A recent study also demonstrated that the CGT mode is an important tool for enhancing the skill of summertime seasonal forecasts for the European sector (Beverley *et al* 2019).

CGT plays an important role in transferring the influence of tropical thermal forcing to the Northern Hemisphere extratropics (Ding *et al* 2011, Lee *et al* 2014). The tropical SST anomaly during developing ENSO summers drives a strong zonally symmetric seesaw pattern in the tropics and extratropics, triggering a tropical–extratropical teleconnection (Ding *et al* 2011). Meanwhile, ENSO may modulate

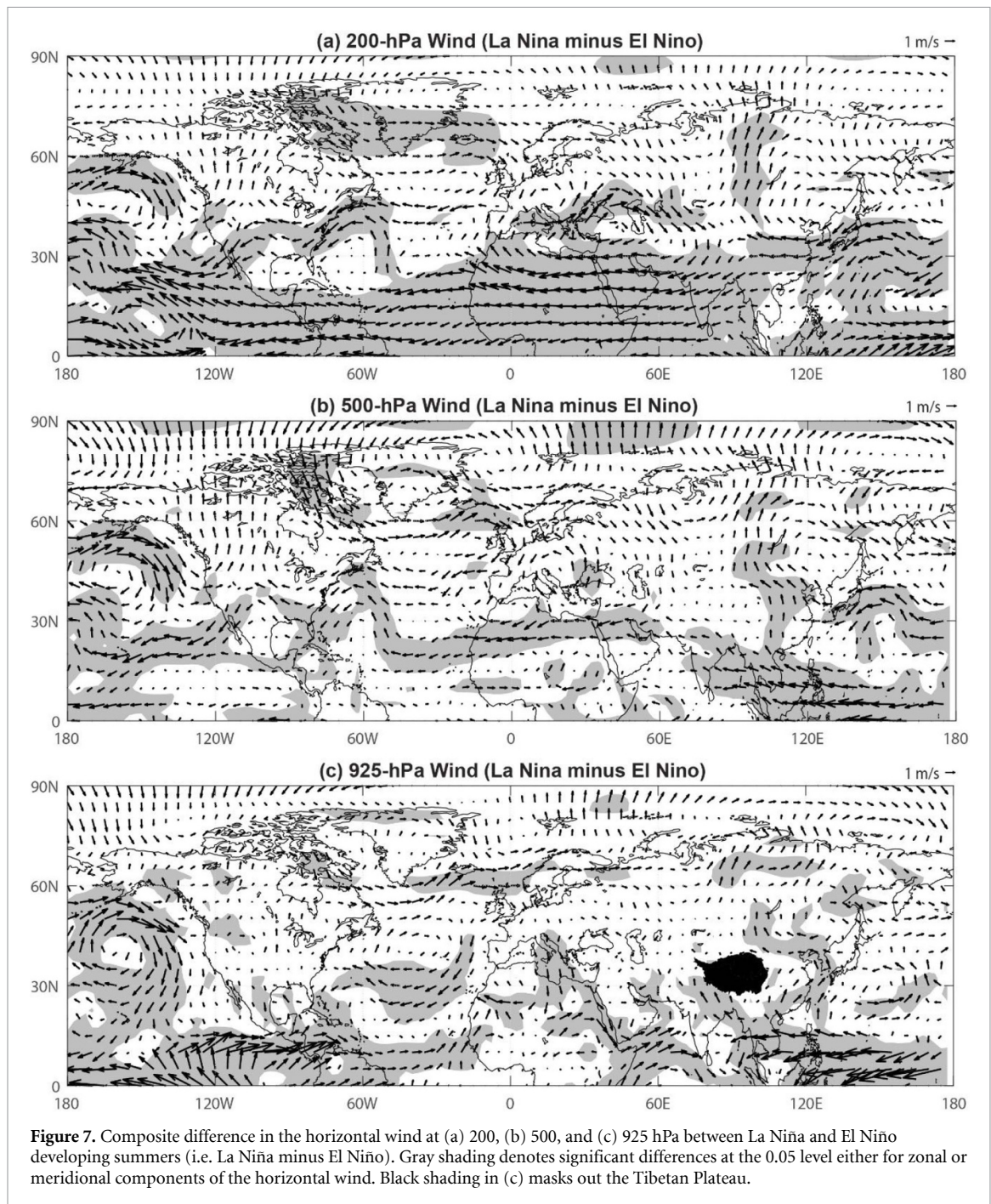


the rainfall anomalies in tropics and the Northern Hemisphere monsoons (e.g. Indian summer monsoon), which in turn acts to excite the wave components of the CGT pattern (Ding and Wang 2005, Ding *et al* 2011). A recent study by Wen *et al* (2019) also suggested that the SST anomalies induce vertical motion-related upper-level vorticity perturbation over the central-eastern tropical Pacific, and this perturbation enables a Rossby wave propagating into the waveguide of the subtropical jet and then to remote mid-latitude regions in the CGT wave train.

The height pattern associated with developing ENSO events at the 500 hPa level (figure 6(b)) is similar to that at 200 hPa. Although the anomalies are slightly weaker at 500 hPa than at 200 hPa, the areas of North America, Central Asia, and Northeast Asia are prominently covered by positive height

anomalies. Slightly enhanced height anomalies at the 925 hPa level prevail over the regions of North Pacific, North Atlantic, and Northeast Asia (figure 6(c)). In some regions such as Central Asia, the sign in geopotential height anomaly shifts from positive in the upper troposphere to negative in the lower troposphere, indicating a baroclinic response (Tang *et al* 2013).

In addition to the responses of anomalous height fields, the wind field is also strongly affected by developing ENSO events (figure 7). During the summer of developing La Niña, anomalous anticyclonic flows are distributed at the middle and upper troposphere over western and eastern coastal regions of North America, Eastern Europe–Central Asia, and Northeast Asia (figures 7(a)–(b)). These anticyclones correspond well with positive height anomaly



centers over the mid-latitudes (figure 6). The enhanced upper-tropospheric height and anomalous anticyclones are favorable for a persistent weather environment (Fink *et al* 2004, Tang *et al* 2013, Lau and Nath 2014), thereby supporting the occurrence of heat extremes in these areas. Also, the anomalous upper-level westerly flow appears along much of higher latitudes, and easterly appears over lower latitudes (figure 7(a)). This pattern suggests a general northward shift of the jet stream in most areas of northern mid-latitudes associated with developing La Niña events. As reported by Wang and Zhang (2002), during a developing La Niña (El Niño), the East Asian trough seems to be shallower (deeper) than normal, and with this abnormal shallowing

(deepening), the upper westerly jet extends poleward (equatorward).

To further elucidate the mechanisms underlying the circulation features, we present geopotential height and wind differences at the 925 hPa level between the La Niña and El Niño developing summers (figures 6(c) and 7(c)). Although the height anomalies at 925 hPa are smaller and less expansive than those at 200 hPa and 500 hPa, the spatial patterns are very similar. An exception is Central Asia, where negative 925 hPa height anomalies are observed. At 925 hPa, anomalous anticyclonic circulations appear over North Pacific, North Atlantic and Europe, and Northeast Asia. These increased (decreased) geopotential height and anomalous anticyclone

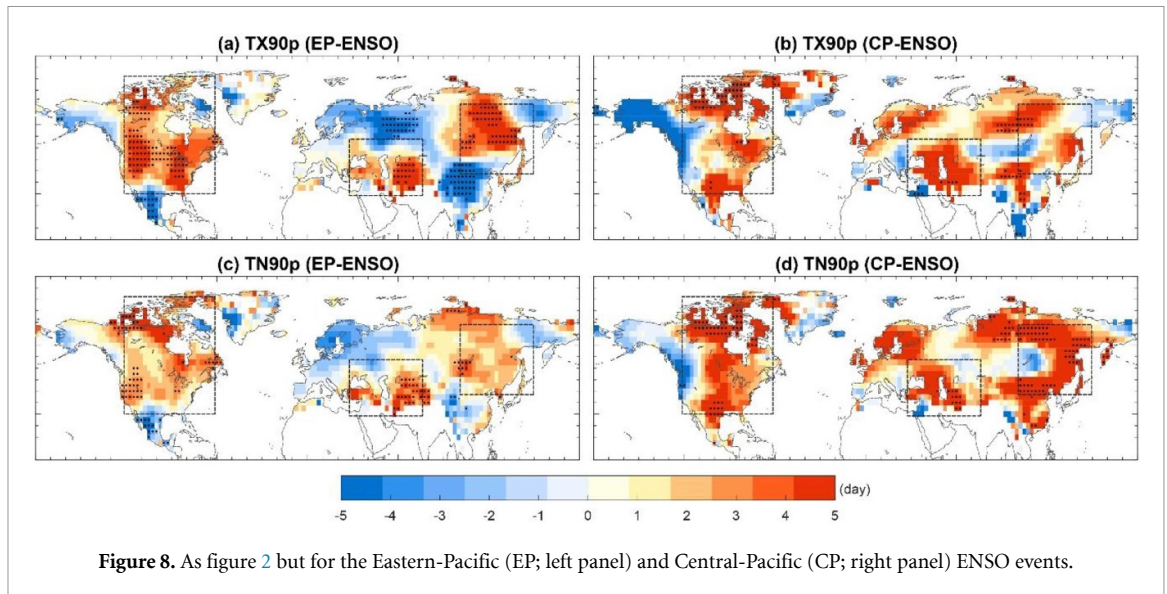


Figure 8. As figure 2 but for the Eastern-Pacific (EP; left panel) and Central-Pacific (CP; right panel) ENSO events.

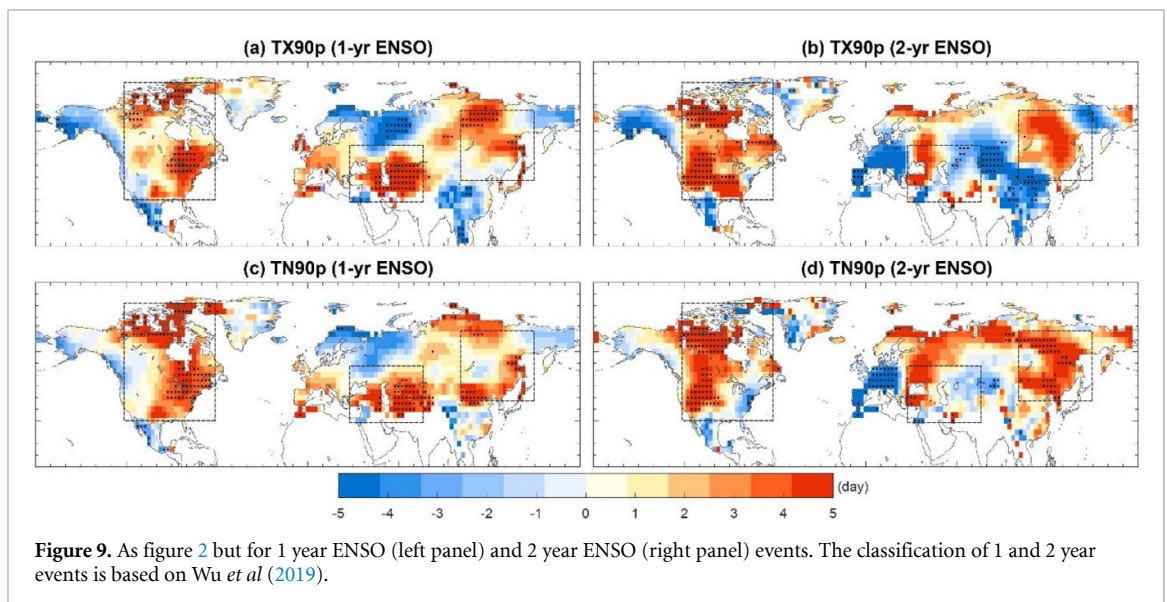


Figure 9. As figure 2 but for 1 year ENSO (left panel) and 2 year ENSO (right panel) events. The classification of 1 and 2 year events is based on Wu *et al* (2019).

(cyclone) at the lower atmosphere in association with developing La Niña (El Niño) forcing can lead to more (less) persistent weather conditions that favor extreme summer heat events in the mid-latitude Northern Hemisphere.

#### 4. Conclusion and discussion

In this study, we demonstrate that there are strong linkages between developing ENSO events and summer weather patterns in northern continents. On the basis of the composite analysis of the summers of developing La Niña and El Niño events, we find that many northern mid-latitude regions (particularly North America, Eastern Europe–Central Asia, and Northeast Asia) experience more (less) frequent summer extreme heat weathers during the La Niña (El Niño) developing phases. These general features are in accord with the association of a CGT pattern with ENSO forcing.

Further examinations of atmospheric circulation changes accompanying ENSO suggest that, during the summer of developing La Niña, the CGT and upper-level flow patterns are characterized by increased geopotential height and anomalous anticyclonic circulations over North Pacific, North America, Eastern Europe–Central Asia, and Northeast Asia. The upper-level jet stream over mid-latitudes is shifted poleward. Such atmospheric circulation changes are associated with more persistent weather conditions that favor extreme summer heat events. Conversely, less frequent heat extremes occur in these areas during the El Niño developing summer due to opposite changes in the atmospheric circulation. Model simulations in previous studies (e.g. Ding *et al* (2011), and Lee *et al* (2014)) also demonstrated that developing ENSO favors the circumglobal teleconnection (CGT) pattern which plays an important role in conveying the influences of tropical SST forcing to remote regions over the extratropical Northern Hemisphere. As our analyses are based on

observational (i.e. GHCNDEX) and reanalysis dataset, it is also of great interest to examine the linkages further in model simulations in future work.

Previous studies show that ENSO events have profound influences on extreme events around the world in the decaying summers (Kenyon and Hegerl 2008, Arblaster and Alexander 2012, Loikith and Broccoli 2014, Lin *et al* 2018, Loughran *et al* 2019, Luo and Lau 2019, Zhao *et al* 2019). For example, Arblaster and Alexander (2012) analyzed both observational data (i.e. HadEX2) and climate model simulations. They suggested that extreme maximum temperatures over Australia, southern Asia, Canada, and South Africa are significantly cooler in decaying La Niña events than in El Niño events; whereas the temperatures over the contiguous United States and southern South America are significantly warmer. The results of our present study extend the scope of these previous studies by demonstrating strong linkages between developing ENSO and summer extreme weather in the Northern Hemisphere.

Recently, the Modoki central Pacific (CP) ENSO characterized by SST anomalies in the tropical central Pacific has attracted attention (Ashok and Yamagata 2009, Lee and McPhaden 2010, Ren and Jin 2011). Compared with the conventional eastern Pacific (EP) ENSO, CP-ENSO has different influences on climate variations in some regions (Kao and Yu 2009, Kim and Yu 2012, Gao *et al* 2020a, Gao *et al* 2020b). Here we follow Ren and Jin (2011), Ren *et al* (2018) and Gao *et al* (2020a) to classify the selected developing ENSO summers into EP and CP types (see also figure 1), and examine the composite difference maps of summer heat extremes for CP-ENSO and EP-ENSO (see figure 8). As figure 8 shows, EP-ENSO and CP-ENSO exhibit a similar spatial pattern of the response of heat extremes in northern midlatitudes. In particular, positive anomalies of hot extremes appear over the regions of North America, Eastern Europe–Central Asia, and Northeast Asia.

In addition to the spatial pattern of ENSO events, different durations of ENSO events have also been noticed in previous studies (Okumura and Deser 2010, Choi *et al* 2013, Wu *et al* 2019). Adopting the definition of Wu *et al* (2019), we classify the selected ENSO years into 1 year and 2 year categories (see their figure 1), and compare the TX90p/TN90p changes associated with these two categories (figure 9). We find that the TX90p/TN90p responses to the two ENSO categories generally exhibit a similar spatial pattern. Some regional differences can also be found. Compared with 2 year ENSO, 1 year ENSO events tend to have stronger influences on TX90p/TN90p over Eastern Europe–Central Asia than 2 year ENSO; whereas, 2 year ENSO poses stronger responses over North America than 1 year ENSO.

Although there is much to learn about the interaction between tropical SST and mid-latitudes, our study provides evidence linking tropical ENSO events

with summer extreme weather in Northern Hemisphere mid-latitudes. The analyses of our study indicate that, in addition to decaying ENSO events, developing ENSO is also an important factor affecting summer extreme heat events in northern continents. SST patterns are often predictable several months ahead and can affect the climate in local and remote regions, thereby the oceanic patterns of climate variability (e.g. ENSO) are an important source of seasonal climate prediction and forecast (Barnston and Smith 1996, Chen *et al* 2011, Patricola *et al* 2017). Our understanding of the linkage between climate extremes and developing ENSO events implies some predictability of the midlatitude climate in the ENSO developing stage from the SST prediction in the coupled ocean-atmosphere-land models and helps to improve the skill in seasonal forecasts and future projections of summer extreme events.

## Acknowledgments

This study is partially funded by the National Natural Science Foundation of China (Grant Nos. 41871029, 41401052). The appointment of M. Luo at Sun Yat-sen University is partially supported by the Pearl River Talent Recruitment Program of Guangdong Province, China (2017GC010634). The authors are very grateful to three anonymous reviewers for their valuable comments and suggestions on the earlier version of the paper.

## Data availability statement

The data that support the findings of this study are openly available. The NCEP/NCAR Reanalysis I dataset is obtained from the NOAA Earth System Research Laboratory at <https://www.esrl.noaa.gov/psd/data/gridded/data.ncep.reanalysis.html>. Summer extreme heat event indices from 1951 to 2019 is from the GHCNDEX dataset available at <https://www.climdex.org/access/gridded/>. The monthly Niño3.4 index is obtained from the NOAA Climate Prediction Center at [http://www.cpc.noaa.gov/products/analysis\\_monitoring/ensostuff/ensoyears.shtml](http://www.cpc.noaa.gov/products/analysis_monitoring/ensostuff/ensoyears.shtml).

## Highlights

- Extreme summer heat events over mid-latitude northern continents are strongly linked to developing La Niña and El Niño events
- More (Less) hot extremes in North America, Eastern Europe–Central Asia, and Northeast Asia occur in La Niña (El Niño) developing summers
- La Niña induces a circumglobal teleconnection pattern with upper high and anticyclone anomalies that favor more persistent weather regimes

## ORCID iD

Ming Luo  <https://orcid.org/0000-0002-5474-3892>

## References

- Alexander L V, Uotila P and Nicholls N 2009 Influence of sea surface temperature variability on global temperature and precipitation extremes *J. Geophys. Res.* **114** D18116
- Arblaster J M and Alexander L V 2012 The impact of the El Niño–Southern Oscillation on maximum temperature extremes *Geophys. Res. Lett.* **39** L20702
- Ashok K and Yamagata T 2009 The El Niño with a difference *Nature* **461** 481–4
- Barnston A G and Smith T M 1996 Specification and prediction of global surface temperature and precipitation from global SST using CCA *J. Clim.* **9** 2660–97
- Barriopedro D and Calvo N 2014 On the relationship between ENSO, stratospheric sudden warmings, and blocking *J. Clim.* **27** 4704–20
- Behera S, Ratnam J V, Masumoto Y and Yamagata T 2013 Origin of extreme summers in Europe: the Indo-Pacific connection *Clim. Dyn.* **41** 663–76
- Beverly J D, Woolnough S J, Baker L H, Johnson S J and Weisheimer A 2019 The northern hemisphere circumglobal teleconnection in a seasonal forecast model and its relationship to European summer forecast skill *Clim. Dyn.* **52** 3759–71
- Chen Y, Randerson J T, Morton D C, Defries R S, Collatz G J, Kasibhatla P S, Giglio L, Jin Y and Marlier M E 2011 Forecasting fire season severity in South America using sea surface temperature anomalies *Science* **334** 787–91
- Choi J Y, Ham Y G and Mcgregor S 2019 Atlantic-Pacific SST gradient change responsible for the weakening of North Tropical Atlantic-ENSO relationship due to global warming *Geophys. Res. Lett.* **46** 7574–82
- Choi K-Y, Vecchi G A and Wittenberg A T 2013 ENSO transition, duration, and amplitude asymmetries: role of the nonlinear wind stress coupling in a conceptual model *J. Clim.* **26** 9462–76
- Deschênes O and Greenstone M 2011 Climate change, mortality, and adaptation: evidence from annual fluctuations in weather in the US *Am. Econ. J.* **3** 152–85
- Ding Q and Wang B 2005 Circumglobal teleconnection in the Northern hemisphere summer *J. Clim.* **18** 3483–505
- Ding Q, Wang B, Wallace J M and Branstator G 2011 Tropical–extratropical teleconnections in boreal summer: observed interannual variability *J. Clim.* **24** 1878–96
- Ding T, Qian W and Yan Z 2010 Changes in hot days and heat waves in China during 1961–2007 *Int. J. Climatol.* **30** 1452–62
- Donat M G, Alexander L V, Yang H, Durrie I, Vose R and Caesar J 2013 Global land-based datasets for monitoring climatic extremes *Bull. Am. Meteorol. Soc.* **94** 997–1006
- Dosio A, Mentaschi L, Fischer E M and Wyser K 2018 Extreme heat waves under 1.5 °C and 2 °C global warming *Environ. Res. Lett.* **13** 054006
- Duchon C E 1979 Lanczos filtering in one and two dimensions *J. Appl. Meteorol.* **18** 1016–22
- Easterling D R, Meehl G A, Parmesan C, Changnon S A, Karl T R and Mearns L O 2000 Climate extremes: observations, modeling, and impacts *Science* **289** 2068–74
- Fink A H, Brücher T, Krüger A, Leckebusch G C, Pinto J G and Ulbrich U 2004 The 2003 European summer heatwaves and drought—synoptic diagnosis and impacts *Weather* **59** 209–16
- Forzieri G, Cescatti A, Silva F B and Feyen L 2017 Increasing risk over time of weather-related hazards to the European population: A data-driven prognostic study *Lancet Planet. Health* **1** e200–e208
- Freychet N, Tett S, Wang J and Hegerl G 2017 Summer heat waves over Eastern China: dynamical processes and trend attribution *Environ. Res. Lett.* **12** 024015
- Gao T, Zhang Q and Luo M 2020a Intensifying effects of El Niño events on winter precipitation extremes in southeastern China *Clim. Dyn.* **54** 631–48
- Gao T, Luo M, Lau N-C and Chan T O, 2020b Spatially distinct effects of two El Niño types on summer heat extremes in China *Geophys. Res. Lett.* **47** e2020GL086982
- Garfinkel C I and Hartmann D L 2007 Effects of the El Niño–Southern Oscillation and the Quasi-Biennial Oscillation on polar temperatures in the stratosphere *J. Geophys. Res.* **112** D19112
- Gasparrini A *et al* 2015 Mortality risk attributable to high and low ambient temperature: A multicountry observational study *Lancet* **386** 369–75
- IPCC (2013) Climate change 2013: the physical science basis. *Contribution of working group I to the fifth assessment report of the Intergovernmental Panel on Climate Change* (Cambridge: Cambridge University Press) pp 1535
- Kalnay E *et al* 1996 The NCEP/NCAR 40-year reanalysis project *Bull. Am. Meteorol. Soc.* **77** 437–71
- Kao H-Y and Yu J-Y 2009 Contrasting Eastern-Pacific and Central-Pacific types of ENSO *J. Clim.* **22** 615–32
- Karori M A, Li J and Jin -F-F 2013 The asymmetric influence of the two types of El Niño and La Niña on summer rainfall over Southeast China *J. Clim.* **26** 4567–82
- Kenyon J and Hegerl G C 2008 Influence of modes of climate variability on global temperature extremes *J. Clim.* **21** 3872–89
- Kim S T and Yu J Y 2012 The two types of ENSO in CMIP5 models *Geophys. Res. Lett.* **39** L11704
- Kosaka Y, Chowdary J S, Xie S-P, Min Y-M and Lee J-Y 2012 Limitations of seasonal predictability for summer climate over East Asia and the northwestern Pacific *J. Clim.* **25** 7574–89
- Kovats R S and Hajat S 2008 Heat stress and public health: A critical review *Annu. Rev. Public Health* **29** 41–55
- Lau N-C and Nath M J 2012 A model study of heat waves over North America: meteorological aspects and projections for the twenty-first century *J. Clim.* **25** 4761–84
- Lau N-C and Nath M J 2014 Model simulation and projection of European heat waves in present-day and future climates *J. Clim.* **27** 3713–30
- Lee J-Y and Ha K-J 2015 Understanding of interdecadal changes in variability and predictability of the northern hemisphere summer tropical–extratropical teleconnection *J. Clim.* **28** 8634–47
- Lee J-Y, Wang B, Seo K-H, Kug J-S, Choi Y-S, Kosaka Y and Ha K-J 2014 Future change of northern hemisphere summer tropical–extratropical teleconnection in CMIP5 models *J. Clim.* **27** 3643–64
- Lee T and Mcphaden M J 2010 Increasing intensity of El Niño in the central-equatorial Pacific *Geophys. Res. Lett.* **37** L14603
- Lin A and Li T 2008 Energy spectrum characteristics of boreal summer intraseasonal oscillations: climatology and variations during the ENSO developing and decaying phases *J. Clim.* **21** 6304–20
- Lin L, Chen C and Luo M 2018 Impacts of El Niño Southern Oscillation on heat waves in the Indochina Peninsula *Atmos. Sci. Lett.* **19** e856
- Liu Q, Zhou T, Mao H and Fu C 2019a Decadal variations in the relationship between the western Pacific subtropical high and summer heat waves in East China *J. Clim.* **32** 1627–40
- Liu S-M, Chen Y-H, Rao J, Cao C, Li S-Y, Ma M-H and Wang Y-B 2019b Parallel comparison of major sudden stratospheric warming events in CESM1-WACCM and CESM2-WACCM *Atmosphere* **10** 679
- Loikith P C and Broccoli A J 2014 The influence of recurrent modes of climate variability on the occurrence of winter and summer extreme temperatures over North America *J. Clim.* **27** 1600–18
- Loughran T F, Pitman A J and Perkins-Kirkpatrick S E 2019 The El Niño–Southern Oscillation’s effect on summer heatwave development mechanisms in Australia *Clim. Dyn.* **52** 6279–300
- Luo M and Lau N-C 2017 Heat waves in southern China: synoptic behavior, long-term change, and urbanization effects *J. Clim.* **30** 703–20

- Luo M and Lau N-C 2019a Increasing heat stress in urban areas of eastern China: Acceleration by urbanization *Geophys. Res. Lett.* **45** 13060–9
- Luo M and Lau N-C 2019b Amplifying effect of ENSO on heat waves in China *Clim. Dyn.* **52** 3277–89
- Ma W, Chen R and Kan H 2014 Temperature-related mortality in 17 large Chinese cities: how heat and cold affect mortality in China *Environ. Res.* **134** 127–33
- Meehl G A and Tebaldi C 2004 More intense, more frequent, and longer lasting heat waves in the 21st century *Science* **305** 994–7
- Okumura Y M and Deser C 2010 Asymmetry in the duration of El Niño and La Niña *J. Clim.* **23** 5826–43
- Oleson K, Monaghan A, Wilhelmi O, Barlage M, Brunsell N, Feddema J, Hu L and Steinhoff D 2015 Interactions between urbanization, heat stress, and climate change *Clim. Change* **129** 525–41
- Patricola C M, Saravanan R and Chang P 2017 A teleconnection between Atlantic sea surface temperature and eastern and central North Pacific tropical cyclones *Geophys. Res. Lett.* **44** 1167–74
- Philippon N, Rouault M, Richard Y and Favre A 2012 The influence of ENSO on winter rainfall in South Africa *Int. J. Climatol.* **32** 2333–47
- Pozo-Vázquez D, Esteban-Parra M, Rodrigo F and Castro-Diez Y 2001 The association between ENSO and winter atmospheric circulation and temperature in the North Atlantic region *J. Clim.* **14** 3408–20
- Rao J and Ren R 2016 Asymmetry and nonlinearity of the influence of ENSO on the northern winter stratosphere: 1. Observations *J. Geophys. Res.* **121** 9000–16
- Rao J and Ren R 2017 Parallel comparison of the 1982/83, 1997/98 and 2015/16 super El Niños and their effects on the extratropical stratosphere *Adv. Atmos. Sci.* **34** 1121–33
- Rao J and Ren R 2020 Modeling study of the destructive interference between the tropical Indian Ocean and eastern Pacific in their forcing in the southern winter extratropical stratosphere during ENSO *Clim. Dyn.* **54** 2249–66
- Ren H-L and Jin -F-F 2011 Niño indices for two types of ENSO *Geophys. Res. Lett.* **38** L04704
- Ren H-L, Lu B, Wan J, Tian B and Zhang P 2018 Identification standard for ENSO events and its application to climate monitoring and prediction in China *J. Meteorol. Res.* **32** 923–36
- Schaller N, Sillmann J, Anstey J, Fischer E M, Grams C M and Russo S 2018 Influence of blocking on Northern European and Western Russian heatwaves in large climate model ensembles *Environ. Res. Lett.* **13** 054015
- Stefanon M, D'Andrea F and Drobinski P 2012 Heatwave classification over Europe and the Mediterranean region *Environ. Res. Lett.* **7** 014023
- Sun X, Renard B, Thyer M, Westra S and Lang M 2015 A global analysis of the asymmetric effect of ENSO on extreme precipitation *J. Hydrol.* **530** 51–65
- Sun Y, Zhang X, Ren G, Zwiers F W and Hu T 2016 Contribution of urbanization to warming in China *Nat. Clim. Change* **6** 706–9
- Tang Q, Zhang X and Francis J A 2013 Extreme summer weather in northern mid-latitudes linked to a vanishing cryosphere *Nat. Clim. Change* **4** 45
- Trenberth K E 1997 The definition of El Niño *Bull. Am. Meteorol. Soc.* **78** 2771–7
- Wang B and Zhang Q 2002 Pacific-east Asian teleconnection. Part II: how the Philippine Sea anomalous anticyclone is established during El Niño development *J. Clim.* **15** 3252–65
- Wang H, Wang B, Huang F, Ding Q and Lee J Y 2012 Interdecadal change of the boreal summer circumglobal teleconnection (1958–2010) *Geophys. Res. Lett.* **39** L12704
- Wang W, Zhou W and Chen D 2014 Summer high temperature extremes in southeast China: bonding with the El Niño–Southern Oscillation and East Asian summer monsoon coupled system *J. Clim.* **27** 4122–38
- Wang W, Zhou W, Wang X, Fong S K and Leong K C 2013 Summer high temperature extremes in southeast China associated with the East Asian jet stream and circumglobal teleconnection *J. Geophys. Res.* **118** 8306–19
- Wen N, Liu Z and Li L 2019 Direct ENSO impact on East Asian summer precipitation in the developing summer *Clim. Dyn.* **52** 6799–815
- Wu B, Zhou T and Li T 2009 Contrast of rainfall–SST relationships in the western North Pacific between the ENSO-developing and ENSO-decaying summers *J. Clim.* **22** 4398–405
- Wu R, Hu -Z-Z and Kirtman B P 2003 Evolution of ENSO-related rainfall anomalies in East Asia *J. Clim.* **16** 3742–58
- Wu X, Okumura Y M and Dinezio P N 2019 What controls the duration of El Niño and La Niña events? *J. Clim.* **32** 5941–65
- Xue F, Dong X and Fan F 2018 Anomalous western Pacific subtropical high during El Niño developing summer in comparison with decaying summer *Adv. Atmos. Sci.* **35** 360–7
- Yeo S-R, Yeh S-W and Lee W-S 2019 Two types of heat wave in Korea associated with atmospheric circulation pattern *J. Geophys. Res.* **124** 7498–511
- Zhao X, Rao J and Mao J 2019 The salient differences in China summer rainfall response to ENSO: phases, intensities and flavors *Clim. Res.* **78** 51–67